Proceedings of 31st International Symposium on Robotics (ISR2000)
Montreal, Qc, Canada, May 14-17, pp. 36-41

Robust Control of a Robot Joint with Hydraulic Actuator Redundancy

Benoit Boulet and Vincent Hayward
McGill University
Research Centre for Intelligent Machines
3480 University Street, Montréal, Québec, Canada H3A 2A7
e-mail: boulet@cim.mcgill.ca, hayward@cim.mcgill.ca

keywords: parallel robot, actuator redundancy, force optimization, load balancing, robust control.

Abstract: A robot joint with two hydraulic actuators, one being redundant, is described. Two methods are proposed for allocating actuation effort in terms of the solutions of minimum-norm problems. In each case, a particular physical interpretation is given. A robust PID controller derived from robust servomechanism theory and a robust controller based on the $\mathcal{H}_\infty$-optimal sensitivity minimization method are designed and experimentally tested. Conclusions are drawn comparing the two approaches.

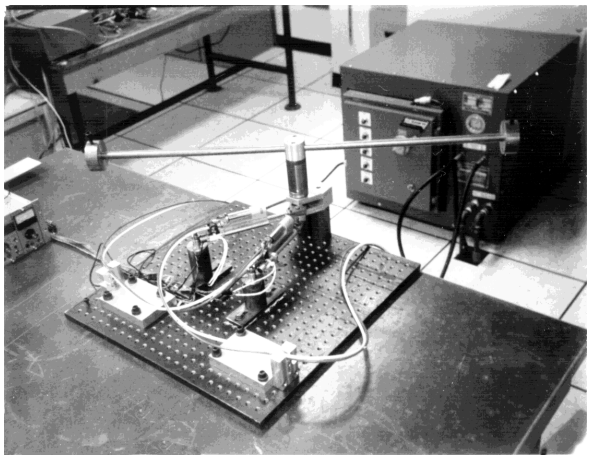

Figure 1: Robot joint prototype

1 INTRODUCTION

Actuator redundancy is a technique that overcomes some of the limitations of joint designs for robot and other mechanically demanding applications. Actuator redundancy can improve the kinematic transfer functions of certain mechanisms, eliminating loci of kinematic singularities, providing ways of evenly distributing stress in a structure, actively canceling backlash in passive joints, increasing efficiency, accuracy, as well as other possibilities [7]. The planar joint prototype powered with two high-performance hydraulic actuators is shown in Figure 1. The actuators are described in detail in [2] and [3]. The kinematic, structural, and dynamic properties of the dual actuator joint are particularly simple, yet, it exhibits all the relevant features of redundantly-actuated parallel mechanisms as introduced above.

Closed-loop stability and performance are properties that should be maintained under a wide range of conditions, including the case with significant uncertainty in the joint and load models. There is some uncertainty in the sensors and actuators dynamics. There is also significant uncertainty related to the task (payload inertia). Finding the best joint angle controller for one single performance criterion is not our concern here, so we restrict our attention to linear time-invariant controllers because of their simplicity.

2 APPROACH

Robust control of uncertain systems has been approached in a variety of ways, leading to theories such as the $\mathcal{H}_\infty$ control theory [10], and the robust servomechanism theory [4]. The approaches differ in the plant models, the uncertainty models, and the performance measures used. These linear robust control methods have been combined with feedback linearization techniques in robotics.

Two robust linear position controllers are designed for the parallel joint, one based on the robust servomechanism theory, and the other based

Proceedings of 31st International Symposium on Robotics (ISR2000)
Montreal, Qc, Canada, May 14-17, pp. 36-41

on the $\mathcal{H}_\infty$ sensitivity minimization method [10]. It is shown that the $\mathcal{H}_\infty$ controller is more robust to variations in the joint's inertia. Position control experiments were conducted and results are presented and compared. It will be concluded that good performance in trajectory tracking can be achieved with a fixed controller for a large range of inertial loading.

The force-controlled nonlinear hydraulic actuators can be considered as linear voltage-to-force transducers, accurate at low frequencies but rolling off with uncertainty at high frequencies. The closed-loop force bandwidth of the actuators was experimentally determined to be between 50Hz for large amplitudes (up to 510N) and 100Hz for small amplitudes (20N), see [3]. The rest of the joint mechanism and its load are approximated by a constant inertia. This is justified by comparing the relative contribution of the moving masses of the linkages to the inertia of the driven load. In addition, since controllers robust to changes in inertia are specifically designed, detailed modeling is unnecessary.

In the next section, basic kinematic properties of the joint needed to design and implement the controllers are derived. Moreover, the actuator load-balancing problem is solved as instances of minimum-norm problems.

3 LOAD BALANCING

The geometry of the robot joint, as shown in Figure 2, is parameterized by three numbers: the separating angle ψ, the crank's arm-length r, and the shortest actuator length k. The position of the joint is described by the angle γ, which once given, determines the variable actuators' lengths ρ_1 and ρ_2 bounded by k and $k+2r$.

A moment applied to the output shaft corresponds to a bending stress in the crank's arm and axial forces in the actuators. The actuators lengths are measured directly. The kinematics of this mechanism are now derived. Posing $\lambda = r + k$:

$$\rho_1 = (\lambda^2 + r^2 - 2\lambda r \cos\gamma)^{1/2} \quad (1)$$

$$\rho_2 = (\lambda^2 + r^2 - 2\lambda r \cos(\psi - \gamma))^{1/2} \quad (2)$$

$$\gamma = \arccos\left((\lambda^2 + r^2 - \rho_1^2)/(2\lambda r)\right) \quad (3)$$

$$\gamma = \psi - \arccos\left((\lambda^2 + r^2 - \rho_2^2)/(2\lambda r)\right) \quad (4)$$

The indeterminacy in the sign of γ is resolved using redundancy in sensing. If ρ_1 is greater than ρ_2, Equation (3) is used, otherwise (4) is used, thus maximizing accuracy. The Jacobian matrix $\boldsymbol{J}$ is

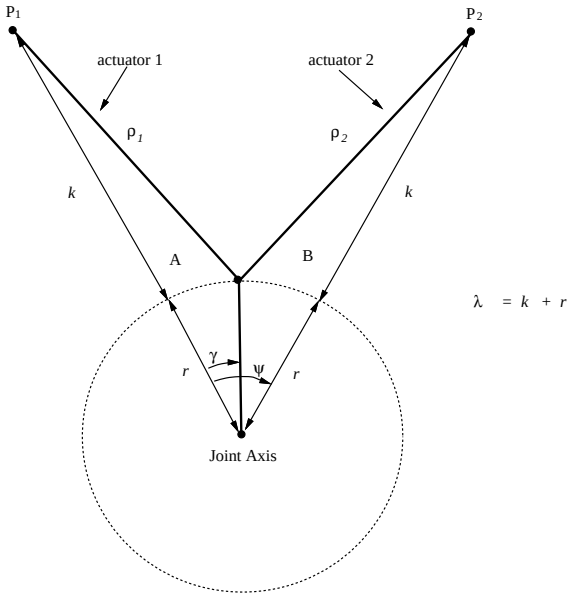

Figure 2: Geometry of the joint

obtained as follows.

$$\dot{\boldsymbol{\rho}} = \boldsymbol{J}\dot{\gamma} \quad (5)$$

$$\tau = \boldsymbol{J}^{\boldsymbol{T}}\boldsymbol{f} \quad (6)$$

$$\text{with} \quad \boldsymbol{J} = \begin{bmatrix} \lambda r \sin\gamma/\rho_1 \\ (-\lambda r \sin(\psi-\gamma))/\rho_2 \end{bmatrix}. \quad (7)$$

where τ is the joint torque and $\boldsymbol{f} = \begin{bmatrix} f_1 & f_2 \end{bmatrix}^T$ is the vector of actuator forces. The rank of the jacobian can be made equal to one irrespective of the joint angle γ with proper values of the mechanical design parameters.

An infinity of solutions for the vector of actuator forces would satisfy Equation (6). We now discuss two methods to compute optimal solutions in the sense of norm minimization, one in Hilbert space, the other in a Banach space. Both methods lead to very simple closed-form solutions suitable for real-time computation. Each of these norms has a simple physical interpretation.

3.1 Minimum 2-Norm Optimal Vector of Forces

The 2-norm optimal vector of forces has a special interpretation: It produces a resultant force that is orthogonal to the moment arm, the latter being aligned with the nullspace of the transposed Jacobian. Hence, the resultant force delivered by the actuators contributes *entirely* to the torque applied at the joint. No stress is generated in the structure as a result of non-working forces. Given the relationship

Proceedings of 31st International Symposium on Robotics (ISR2000)
Montreal, Qc, Canada, May 14-17, pp. 36-41

between τ and $\boldsymbol{f}$, the optimal minimum-norm vector $\tilde{\boldsymbol{f}}$ that satisfies it when the norm is chosen to be the usual Hilbert space norm $\|\boldsymbol{f}\| = (f_1^2 + f_2^2)^{1/2}$ is obtained by using the pseudo-inverse of the transposed Jacobian $\boldsymbol{J^T}$. This expression is computationally efficient:

$$\tilde{\boldsymbol{f}} = \boldsymbol{J}(\boldsymbol{J^T J})^{-1}\tau = \frac{\tau}{j_1^2 + j_2^2}\begin{bmatrix} j_1 \\ j_2 \end{bmatrix}. \qquad (8)$$

3.2 Minimum ∞-Norm Optimal Vector of Forces

The ∞-norm optimal solution has an altogether different interpretation. It minimizes the maximum absolute value of the actuator forces and can therefore be regarded as a way to reduce stress in the actuators, rather than in the structure as it is the case with the 2-norm. Alternatively, it can be regarded as a way to maximize the output torque, given limits in the actuators. The ∞-norm solution vector has forces that are equal in magnitude, and that magnitude is minimal. The minimum-norm optimization problem is formulated in a Banach space with the norm $\|\boldsymbol{f}\|_\infty = \max(|f_1|,\ |f_2|)$. The derivation of the optimal vector can be carried out with the theory of dual Banach spaces, but is omitted here (see [2]). The minimum ∞-norm vector is given by:

$$\tilde{\boldsymbol{f}} = \frac{\tau}{|j_1| + |j_2|}\begin{bmatrix} \mathrm{sgn}(j_1) \\ \mathrm{sgn}(j_2) \end{bmatrix}, \qquad (9)$$

where $\mathrm{sgn}(\cdot)$ has its usual definition. This expression is very simple and can be easily computed in real time.

3.3 Design of a Range of Solutions

It is sometimes desirable to apply a pre-load force in a joint, e.g., to eliminate backlash. This can be accomplished by using a force vector lying in the nullspace of $\boldsymbol{J^T}$. Such a vector would be aligned with the moment arm and thus would not contribute to the movement of the joint. It can be expressed as a unit vector pointing outward:

$$\boldsymbol{n} = \begin{cases} [j_2(j_1^2 + j_2^2)^{-1/2} & -(1 + j_2^2/j_1^2)^{-1/2}]^T, \gamma > 0 \\ [-(1 + j_1^2/j_2^2)^{-1/2} & (1 + j_2^2/j_1^2)^{-1/2}]^T,\ \gamma \le 0 \end{cases} \qquad (10)$$

A pre-load force $F_{pl}\boldsymbol{n}$ can be added to the 2-norm optimal vector $\tilde{\boldsymbol{f}}$. It should be noted that the ∞-norm optimal vector of forces cannot be used for that purpose. However, a range of solutions can be designed by splitting the desired output torque into two additive desired torques. By adjusting the relative weight of each solution, multiple criteria can be traded off at a low computational cost.

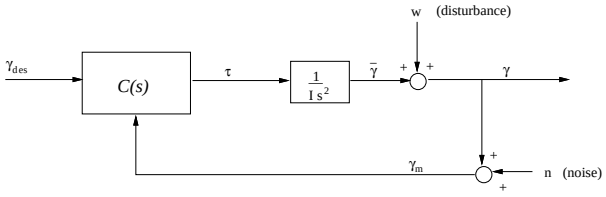

Figure 3: Block diagram of closed-loop system

4 JOINT ANGLE CONTROL

Two approaches are now investigated for robust linear control of the joint angle. Unmodeled linear and nonlinear dynamics, disturbances and variations in system parameters form the uncertainty, and the robustness and disturbance rejection properties of the two control laws should reduce its effect. We consider the case where the redundant revolute joint is carrying a load of inertia I:

$$I\ddot{\gamma} = \tau. \qquad (11)$$

4.1 PID Controller Based on Robust Servomechanism Theory

Assume we only have an estimate $\hat{I}$ of the joint's inertia. The goal is to drive the system so as to track the reference input $\gamma_{des}(t)$ and to reject a possibly persistent disturbance w with uncertainty in the knowledge of the system's inertia and measurement noise (known as the robust servomechanism problem). The internal model principle used in robust servomechanism theory states that a control system is structurally stable (meaning that it is robust to small perturbations in the state-space matrices) only if the controller utilizes feedback of the regulated variable, and incorporates in the feedback a suitably reduplicated model of the exogenous signals [6]. Kuo and Wang [8] demonstrated the usefulness of this principle for robot control when the uncertainty is assumed to be constant ($\dot{e} = 0$) but of unknown magnitude. In this case, the resulting controller is just a classical PID controller, that is, an integral term is added to the usual state feedback controller [5]. Referring to Figure 3 for the notation and following [8], we first apply a state feedback with the proportional and derivative gains K_p and K_d to Equation (11):

$$I\ddot{\bar{\gamma}} = \hat{I}(-K_d\dot{\gamma}_m - K_p\gamma_m + K_p u). \qquad (12)$$

where $\ddot{\bar{\gamma}}$ is the joint angular acceleration before the output disturbance $w(t)$ is added to it. The reference trajectory $\ddot{\gamma}_{des}, \dot{\gamma}_{des}, \gamma_{des}$ implicitly defining u_d

is included, yielding:

$$K_p(u-u_d) = \frac{I}{\hat{I}}\ddot{\gamma} - \ddot{\gamma}_{des} + K_d(\dot{\gamma}_m - \dot{\gamma}_{des}) + K_p(\gamma_m - \gamma_{des}). \tag{13}$$

Define $y = \gamma - \gamma_{des}$ as the tracking error and $v = u - u_d$ as the input from the robust part of the controller, and let $I = \hat{I} + \Delta I$. We have:

$$\ddot{y} + K_d\dot{y} + K_p y = K_p v - e. \tag{14}$$

Where the uncertainty e is given by

$$e = K_d\dot{n} + K_p n - \frac{I}{\hat{I}}\ddot{w} + \frac{\Delta I}{\hat{I}}\ddot{\gamma}. \tag{15}$$

This tells us that for a small ΔI and low-power noise, a slowly-varying e implies that the disturbance w is also slowly-varying, since $\ddot{w}$ must have its energy at low frequency. The assumption that e be constant may be justified for slowly-varying disturbances as well, which for example may be due to friction. In other words, integral control also works well for slowly-varying uncertainty. The rest of the design of the "robust part" can be carried out in the augmented state space $\mathbb{R}^3$ with a second set of state feedback gains $\{K_i\}_{i=1}^3$. The combination of these gains with the initial PD gains yields the PID control law:

$$\tau = \hat{I}[\ddot{\gamma}_{des} + \tilde{K}_p(\gamma_{des} - \gamma_m) + \tilde{K}_d(\dot{\gamma}_{des} - \dot{\gamma}_m) \tag{16}$$

$$+\tilde{K}_i \int_0^t (\gamma_{des}(\lambda) - \gamma_m(\lambda))d\lambda] \tag{17}$$

The gain margin obtained with this PID controller is about -18dB, i.e., instability occurs when the gain is *decreased*. The phase margin is 70°. Therefore the feedback system should have robustness against unmodeled phase lag, but not to uncertainty in the joint's inertia, especially if it is underestimated.

4.2 An $\mathcal{H}_\infty$-Optimal Robust Controller

The second approach investigated is the $\mathcal{H}_\infty$ sensitivity minimization method which originated in the work of Zames and Francis [10]. This corresponds to a minimax problem in which the maximum value of the weighted sensitivity on the $j\omega$-axis is minimized. The sensitivity function

$$S(s) = \frac{1}{1 + C(s)G(s)} \tag{18}$$

bears this name because it is equal to the relative change of the closed-loop transfer function from the reference to the output, to a relative change in the loop gain $L(s) := C(s)G(s)$. The transfer function from w to γ is also equal to the sensitivity function. Thus we see that minimizing the (weighted) sensitivity offers two advantages: it desensitizes the system from variations in the loop gain, and it attenuates the effect of the output disturbance [10]. The $\mathcal{H}_\infty$ controller will guarantee good robustness and good output disturbance rejection for finite-energy or finite-power disturbances $w(t)$.

The following interpolation condition is required for internal stability of the closed-loop system: Since the plant $G(s)$ has a double pole at the origin, $S(s)$ must have a double zero at the same location. We pick a minimum-phase, proper, rational weighting function $W(s)$ and we seek to minimize the $\mathcal{H}_\infty$ norm of the weighted sensitivity $S(s)W(s)$ over all linear time-invariant controllers $C(s)$:

$$\min \|SW\|_\infty = \min \sup_\omega |S(j\omega)W(j\omega)|. \tag{19}$$

We have to use a weighting function because for a strictly proper plant $G(s)$ such as our robot joint, the $\mathcal{H}_\infty$ norm of the sensitivity is always greater or equal to 1 [10]. The weighting function can make $|S(j\omega)|$ small at low frequencies by choosing a large $|W(j\omega)|$ at those frequencies.

We now design an optimal sensitivity by picking a suitable weighting function $W(s)$. First, notice that $|W(j\omega)|$ inverts $|S(j\omega)|$ and that $W(s)$ must have two poles at $s = 0$ since the plant model is $G(s) = 1/\hat{I}s^2$. Zeros can be selected for $W(s)$ which become the closed-loop poles. After a few trials, we chose $W(s)$ such that low-frequency output disturbances could be rejected and perturbations of the loop gain at low frequencies could be tolerated without inducing instability (stability robustness).

$$W(s) = \frac{(s/\omega_a + 1)^3}{s^2(s/b + 1)}. \tag{20}$$

The corresponding optimal sensitivity is

$$S(s) = \frac{ks^2(s/b + 1)}{(s/\omega_a + 1)^3}. \tag{21}$$

The gain k is now adjusted such that $S(j\omega) \to 1$ as $\omega \to \infty$ to make sure that the magnitude $|H(j\omega)|$ of the complementary sensitivity function $H(s) = 1 - S(s)$ mapping γ_{des} to γ rolls off at high frequencies as fast as the second-order plant. Thus the actuators will not be delivering too much power at high frequencies: $\lim_{\omega\to\infty} S(j\omega) = (k\omega_a^3)/b = 1$, so that $k = b/\omega_a^3$.

We now calculate the controller $C(s)$ after selecting $b = 3\omega_a$ and $k = 3/\omega_a^2$.

$$C(s) = \frac{H(s)}{G(s)S(s)} = \frac{\hat{I}\omega_a^2(3s/\omega_a + 1)}{3(s/3\omega_a + 1)} \tag{22}$$

Proceedings of 31st International Symposium on Robotics (ISR2000)
Montreal, Qc, Canada, May 14-17, pp. 36-41

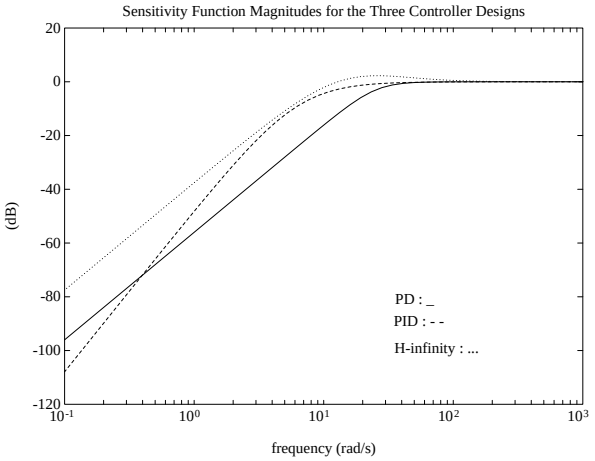

Figure 4: Sensitivity functions

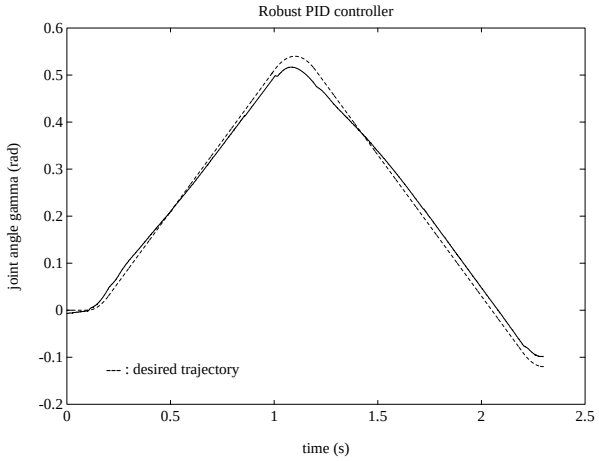

Figure 5: Joint angle response with PID controller, overestimated inertia

$C(s)$ turns out to be a classical lead controller. Of course, the structure of the controller always depends on the choice of the weighting function $W(s)$, which is the real design parameter.

We set $\omega_a = 15$ rd/s in the controller. The phase margin is a little more than 50° while the gain margin is infinite, showing good "classical" robustness properties. More importantly, the optimal $S(s)$ maximizes the stability robustness margin $1+L(j\omega)$ to arbitrary stable loop gain perturbations $\Delta(s)$ with magnitudes bounded by $W(j\omega)$ on the imaginary axis.

The sensitivity magnitudes of the two robust controller designs and of a third baseline PD controller are plotted in Figure 4. It can be seen that, paradoxically, the $\mathcal{H}_\infty$-optimal controller yields the largest sensitivity magnitude of the three designs. This is due to its low bandwidth limited to $\omega_a = 15$ rd/s to prevent the onset of nonlinear instability in the hydraulic actuators. More interestingly, even though the $\mathcal{H}_\infty$-optimal design displays the largest sensitivity magnitude, it is on the other hand more robust to variations in the joint's inertia than the PID design because it has an infinite gain margin. This is an important remark since robustness is an important specification in many robotics applications. Thus, the sensitivity obtained with the $\mathcal{H}_\infty$ controller seems to offer a better robustness/performance tradeoff. Note that recent results in robust control [1] suggest that such a robustness/performance tradeoff would be best addressed by the $\mathcal{H}_\infty$-theory-based μ-synthesis approach in which both objectives are optimized concurrently.

5 EXPERIMENTAL RESULTS

Two control experiments were conducted to evaluate and compare the robustness of the PID and the $\mathcal{H}_\infty$-optimal controllers for an overestimated inertia, that is $I = 0.36$ while $\hat{I} = 0.71$. Feedforward of the desired angular acceleration was used with the $\mathcal{H}_\infty$-optimal controller for a better comparison with the PID controller. The closed-loop joint angle trajectories are plotted in Figures 5 and 6. The $\mathcal{H}_\infty$-optimal controller offered more robustness and better tracking performance under these conditions. The minimum 2-norm vector of actuator forces was implemented in both cases for load balancing. Another experiment with an underestimated inertia $\hat{I} = 0.2$ while $I = 0.71$ showed that tracking performance of the PID controller deteriorated significantly, as expected from the negative gain margin [2].

6 CONCLUSION

We presented the main kinematic and dynamic control issues associated with a redundant, parallel robot joint with hydraulic actuators. It was suggested to use redundancy in sensing and actuation to increase the accuracy of the joint, to minimize internal stress with the minimum 2-norm vector of actuator forces, or to maximize torque with the minimum ∞-norm vector.

Two robust controllers were designed and experimentally tested. The PID controller showed reasonable tracking performance, but it was not as robust as the $\mathcal{H}_\infty$ lead controller when bad estimates of the joint's inertia were used. The angle

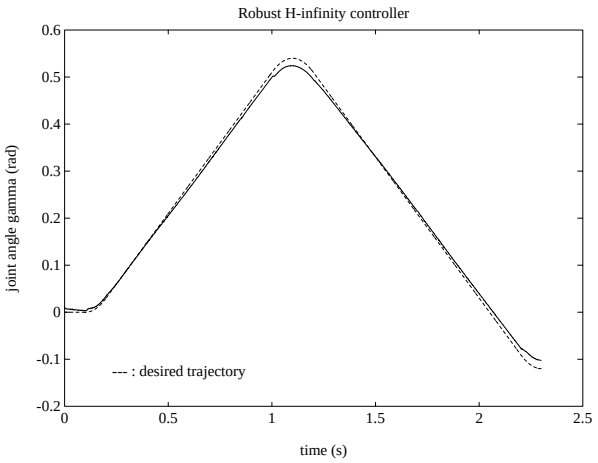

Figure 6: Joint angle response with $\mathcal{H}_\infty$ controller, overestimated inertia

response of the $\mathcal{H}_\infty$-optimal control system satisfactorily tracked the desired joint angle trajectory.

7 ACKNOWLEDGMENT

Support from Canada's IRIS and NSERC and from Québec's FCAR is gratefully acknowledged.

References

[1] Balas, G.J., Doyle, J.C., Glover, K., Packard, A., Smith, R.S., *μ-Analysis and Synthesis Toolbox: User's Guide*. The Mathworks Inc., 1991.

[2] Boulet, B., *Modeling and Control of a Robotic Joint with In-Parallel Redundant Actuators*. M. Eng. Thesis, Dept. of Electrical Engineering, McGill University, 1992, 139 pages.

[3] Boulet, B., Daneshmend, L.K., Hayward, V., Nemri, C., Characterization, Modeling, and Identification of a High Performance Hydraulic Actuator For Robotics. *Experimental Robotics II, The Second International Symposium*, Toulouse, France, June 25-27. Lecture Notes in Control and Information Sciences, R. Chatila, G. Hirzinger (Eds), Springer-Verlag, 1993.

[4] Davison, E.J., Ferguson, I.J., The Design of Controllers for the Multivariable Robust Servomechanism Problem Using Parameter Optimization Methods. *IEEE Transactions on Automatic Control*, Vol. AC-26, No. 1, February 1981.

[5] Desa, S., Roth, B., Synthesis of Control Systems for Manipulators Using Multivariable Robust Servomechanism Theory. *The International Journal of Robotics Research*, Vol. 4, No. 3, Fall 1985.

[6] Francis, B.A., Wonham, W.M., The Internal Model Principle of Control Theory. *Automatica*, Vol. 12, pp. 457-465, 1976.

[7] Hayward, V., Design of hydraulic robot shoulder based on combinatorial mechanism. *Experimental Robotics III: The 3rd International Symposium*, Kyoto, Japan, October 28-30. Lecture Notes in Control and Information Sciences, T. Yoshikawa, F. Miyazaki (Eds), Springer-Verlag, 1994.

[8] Kuo, C.-Y., Wang, S.-P. T., Robust Position Control of Robotic Manipulator in Cartesian Coordinates. *IEEE Transactions on Robotics and Automation*, Vol. 7, No. 5, October 1991.

[9] Spong, M.W., Vidyasagar, M., *Robot Dynamics and Control*. New-York: John-Wiley & Sons, 1989.

[10] Zames, G., Francis, B.A., Feedback, Minimax Sensitivity, and Optimal Robustness. *IEEE Transactions on Automatic Control*, Vol. AC-28, No. 5, May 1983.